GALACTIC PHASE SPACES

DALIA CHAKRABARTY*
Department of Statistics, University of Warwick,
Coventry CV4 7AL, U.K.
*E-mail: d.chakrabarty@warwick.ac.uk
Proceedings of Workshop Science: IMAGe IN AcTION,
organised by the Inernational Consortium of Interdisciplinary Sciences,
at the Ettore Majorana Foundation and Centre for Scientific Culture,
Erice, Sicily, April 15-22, 2011

December 15, 2011

Abstract: Galaxies are argued to manifest complexity, thereby contradicting models of smooth parametric galactic phase space densities. An estimation of chaos in models of our galaxy is forwarded to suggest strength and possible causes of non-linearities in phase space. A Bayesian nonparametric methodology that is designed to acknowledge uncertainties in measured data, when applied to an observed external galaxy, indicates a non-linear galactic phase space density that could result from a bistable system potential. The effect of such a phase space structure on the inverse modelling of phase space data is discussed.
Keywords: Non-linear dynamics; Hypothesis testing; Bayesian non-parametrics.

1 Introduction

A dynamical system is given by its phase space W that is marked by an evolution function $g(\mathbf{w}, t)$ that determines system evolution with time t ($t \in T$). Thus, in general $g : T \times W \longrightarrow W$. Thus, characterisation of the dynamical system would entail estimation of the *pdf* of its phase space $f(\mathbf{w}, t)$ and of $g(\mathbf{w}, t)$, given the available information. In the treatment of astronomical systems - such as galaxies - as non-dissipative dynamical systems, the approximation of the stellar fluid as collisionless is invoked at the very outset.

We assume our astronomical dynamical system as Hamiltonian, and write $g : \mathbb{R}^3 \longrightarrow \mathbb{R}^3$. The spatial coordinates $\mathbf{x} \in \mathbb{R}^3$ and velocities $\mathbf{v}$ ($\mathbf{v} = \dot{\mathbf{x}}$) of all system particles are in W. We also assume that the system has reached stationarity, allowing us to write the *pdf* of W as $f(\mathbf{w})$. The information that is available for the estimation of the phase space density structure and the evolution function can be data of certain phase space coordinates of individual system particles, sampled from a sub-manifold U in W ($\{\mathbf{u}_k\}_{k=1}^N$, where $U \subseteq W$), and/or the observable function $\Psi(\mathbf{u})$. It is the nature of galactic observations that constrain $\mathbf{u}_k$ to $x_1^{(k)}, x_2^{(k)}, v_3^{(k)}$, where $x_1^{(k)}, x_2^{(2)}$ are the coordinates of the k^{th} particle in the image of the system and $v_3^{(k)}$ is the component of $\mathbf{v}_k$ along the line that connects the observer to the k^{th} particle.

The other idiosyncrasy of galaxies is that for such a gravitational system, $g(\mathbf{x})$ is the gravitational field due to all the gravitating matter in the system and is an expression of the gravitational mass density $\rho(\mathbf{x})$: $\nabla \cdot g(\mathbf{x}) = -4\pi G\rho(\mathbf{x})$, where G is the (known) Universal Gravitational constant. The main contributor towards $\rho(\mathbf{x})$ is the dark matter constituent of the system; such dark matter density cannot be observed photometrically since dark matter neither emits nor reflects light, Thus, in place of the more readily available, photometic astronomical observations, we need to inversely model the effects of the total gravitating mass of a galaxy, in order to estimate $\rho(\mathbf{x})$. It may be mentioned that once $\rho(\mathbf{x})$ - and thereby $g(\mathbf{x})$ - is estimated, the evolution of a sample of phase space coordinates can be computed, by plugging in $g(\mathbf{x})$ in Newton's or Einstein's equations of motion. The estimation of such evolution is uncertain insofar as the probabilistic nature of the estimate of $\rho(\mathbf{x})$, i.e. $\hat{\rho}(\mathbf{x})$, is concerned.

In this paper, we explore the estimation of the total gravitational mass density of galaxies, using inverse modelling of the aforementioned "effect"s of galactic gravitational mass. Importantly, the focus of this paper is the effect of non-linearities in $\rho(\mathbf{x})$ and $f(\mathbf{w})$, on the estimation of macroscopic system parameters. In particular, we will examine the effect of chaoticity - brought about by non-linearities in $\rho(\mathbf{x})$ - on galactic relaxation, using the Milky Way as an example. Once the possibility of a multimodal, non-linear galactic phase space density is demonstrated, we will indicate the fundamental risk involved in the estimation of $\rho(\mathbf{x})$ using kinematic data, when the galactic phase space is such.

2 Phase space of the Milky Way

Traditionally, galaxies are treated as built of regular orbits, evolving towards an integrable potential. If this were true, it would indeed be very difficult to explain how - as is typically considered in statistical mechanics - chaotic mixing could have brought the system to the current equilibrium state. Thus, it was considered interesting to test for the chaos-inducing efficiency in a galactic model that is initially based on regular orbits, exhibiting a uniformly distributed phase space structure, and then quantify the relative strength of chaoticity. If such chaoticity is identified, its source is sought - stochasticity in rapidly changing potential as distinguished from resonance-coupling effects - in our own galaxy (Chakrabarty 2007). A useful corollary of such a pursuit is estimation of some Milky Way parameters.

Here we discuss the estimation of relevant Milky Way parameters $S \in \mathbb{R}^n$ in general, (with n=2 in Chakrabarty, 2007), given the velocity data of stars in our galaxy, from within an ϵ neighbourhood of the Sun, $\mathcal{D} = \{v_i\}_{i=1}^N$. It is of importance to appreciate that the estimated spatial location of us - the observer of this data set, is very well approximated by the location of Sun on the Milky Way disc, on astronomical scales. In fact, given the near isotropic sampling around the Sun, if $\epsilon \ll R_\odot$, where $R_\odot$ is a fiduciary value for the radial location of the Sun w.r.t. the Galactic centre (viz. the IAU standard value that we want to improve upon), *the location of the Sun can be approximated as a summary of the distribution of the locations of the stars in this observed sample.* This inequality does hold for the data used in Chakrabarty (2007) in which $\epsilon/R_\odot \approx 0.0125$.

Our estimate for S is $\mathbf{s}_i$, following the identification of the simulated phase space density $\nu(\mathbf{w}|\mathbf{s}_i)$ that offers "maximal" support to the hypothesis that $\mathcal{D} \sim \nu(\mathbf{w}|\mathbf{s}_i)$, $i = 1, \ldots, N_{sim}$, where there are N_{sim} number of simulated phase space densities generated (discussed in details in Section 2.2).

2.1 Simulating phase space data

In Chakrabarty (2007), the Milky Way is modelled as an axisymmetric disc galaxy. Thus, the modelling is done on a 2-D disk, i.e. $\mathbf{x} = (x_1, x_2)^T$ where $x_1 = R\cos\phi$ and $x_2 = R\sin\phi$, where R and ϕ are the radial and azimuthal co-ordinates. In this example about our galaxy, given that the particle velocities are measured w.r.t. the Sun, i.e. we work with the heliocentric particle velocity $\mathbf{v_r} = (U, V)^T$. The solar velocity is considered known within uncertainties offered in astronomical literature.

A sample of phase space coordinates $\{\mathbf{w_0}\}$, simulated from a realistic phase space density $f(\mathbf{w})$ at $t = 0$, is evolved in a parametric gravitational field that models the background axisymmetric Galactic gravitational field $g_0(R)$, perturbed by the non-axisymmetric, perturbing fields $(g_b(R, \phi - \Omega_b t)$ and $g_s(R, \phi - \Omega_s t))$ of two perturbers that model two rotating structural features of the Milky Way disk, namely the bar and the spiral pattern. Here the bar (and spiral) is rotating with frequency Ω_b (and Ω_s), so that the rotation induces an extra azimuth of $\Omega_b t$ in time t. The net gravitational field that the galactic particles evolve in is then $g(R, \phi, t|\Psi)$ where Ψ represents the fixed model parameters including perturbation strengths, spiral details, etc.

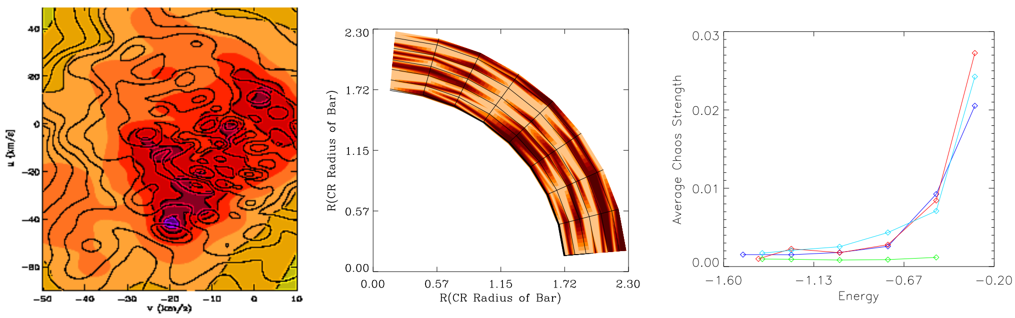

Figure 1: *Left:* The velocities recorded in the ij^{th} $s_1 - s_2$ cell are used to estimate the ij^{th} simulated *pdf* of $U - V$ space that is overlaid in solid black contour lines over $\nu_0(U, V)|\mathcal{D}$ (in contours in grayscale). The non-linear distribution of probability mass is evident in both density structures. *Middle:* Distribution of the support in data $\mathcal{D}$, to the null that the observed data are drawn from the ij^{th} simulated phase space density, as p-value of the test statistic - shown in gray-scale over ranges of s_1 and s_2 used in Chakrabarty (2007). *Right:* Strength of chaos in resonance overlap model (in medium grey) and in models in which the resonances due to the 2 perturbers occur outside respective resonance widths (in light grey and black), as distinguished from Milky Way model missing contribution from the perturbing potential marked by a high spatial gradient (in faint grey at the lowest chaos strengths at all energies); from Chakrabarty & Sideris (2008).

2.2 Generating the simulated phase space densities

At the end of the simulation time, orbits are recorded stroboscopically in a frame that rotates with the bar, at times when $(\Omega_b - \Omega_s)t$=0. By "orbits" is implied the stellar phase space coordinates R, ϕ, U, V values at a given t. If the estimation of the system parameter S is sought, then the recorded orbits are put on a regular $S_1 - S_2 - \ldots - S_m$ grid, where $m = \dim(\mathbf{s})$. Chakrabarty (2007) sought estimates for 2 components of the S vector, the radial (S_1) and azimuthal (S_2) locations of the observer, (i.e. the Sun), with $s_1 = 0$ at the Galactic centre (GC) and $s_2 = 0$ along the bar major axis. Then, the recorded orbits are placed in a regular polar $S_1 - S_2$ grid, with bin widths δR, $\delta\phi$. If a sample of stars is recorded in the ij^{th} $S_1 - S_2$ bin then these stars have spatial coordinates $\{R_k, \phi_l\}_{k=i-1,l=j-1}^{k=i,l=j}$ and will have a summary spatial location within this bin. So, if this sample were the observed sample, then the solar location from which this sample is observed, must be within this bin and can be approximated as the centroid of this bin (see Section 2); here $i = 1, \ldots, i_{max}$, $j = 1, \ldots, j_{max}$, $i_{max} = (R_{max} - R_{min})/\delta R$, $j_{max} = (\phi_{max} - \phi_{min})/\delta\phi$.

Discrete $U - V$ data recorded in each $S_i - S_j$ cell are noted, ($\forall i = 1, \ldots, i_{max}$, $j = 1, \ldots, j_{max}$). The *pdf* of $U - V$ space, for the i^{th} value of S_1 and j^{th} value of S_2 is $\nu(U, V | s_1^{(i)}, s_2^{(j)})$, abbreviated as $\nu_{ij}(U, V)$. Then $\nu_{ij}(U, V)$ is estimated using these simulated $U - V$ data and a kernel density estimation technique that employs an adaptive, bivariate Gaussian kernel. The density estimation is motivated by the bandwidths used for the estimation of the density $\nu_0(U, V)$ from the observed data $\mathcal{D}$.

2.3 Testing

Thus, we have $R_{max} \times \phi_{max}$ number of $S_1 - S_2$ bins, and a simulated density at each bin. To test if $\{U_0^{(i)}, V_0^{(i)}\}_{i=1}^{N} \equiv \mathcal{D}$ is sampled from $\nu_0(U, V)$, Chakrabarty (2007) tested for the null $H0 : \nu_0(U, V) = \nu_{ij}(U, V)$. To test for this null, a test statistic $\mathcal{S}_{ij}$ is defined in the ij^{th} $S_1 - S_2$ bin, (with the aim that the null should be rejected for low p-values), $\forall\, i, j$. We say $\mathcal{S}_{ij} := \mathcal{L}_{ij}^{-1}$ where $\mathcal{L}_{ij}$ is the likelihood, i.e $\mathcal{L}_{ij} = \prod_{q=1}^{N_{ij}} \nu_{ij}(U_q, V_q)$, where heliocentric velocities of N_{ij} stars are recorded in the ij^{th} $S_1 - S_2$ bin, $i = 1, \ldots, i_{max}$, $j = 1, \ldots, j_{max}$. This definition of the likelihood assumes that the data are $i.i.d$ inside each $S_1 - S_2$ bin. The p-value for the ij^{th} bin is $\alpha_{ij} = \Pr(\mathcal{S}_{ij} \geq \mathcal{S}_0 | H0)$ where $\mathcal{S}_0^{-1} := \prod_{i=1}^{N} \nu_0(U_0^{(i)}, V_0^{(i)})$. In the context of this nonparametric inference, α_{ij} is calculated empirically, by drawing N_{tot} number of random (U, V) samples (of size N) from ν_{ij}; if for N_{great} of these N_{tot} samples, the sample test statistic exceeds $\mathcal{S}_0$, then $\alpha_{ij} = N_{great}/N_{tot}$.

We note the i, j for which α_{ij}=1, are recorded: $\{s_1^{(m)}, s_2^{(n)}\}_{m=1,n=1}^{m_{max},n_{max}}$, $m_{max} \leq R_{max}$, $n_{max} \leq \phi_{max}$. s_1 and s_2 in these ranges correspond to the observer locations at which the best support for the null is recovered - these ranges are then advanced as the interval estimates for the solar location.

3 How much chaos?

The frequencies Ω_s and Ω_b affect the degree of non-linearity in the solar neighbouhood by controlling the locations at which resonances due to the spiral and the bar respectively occur. Now, overlap of two major resonances implies the onset of global chaos. As the relative spatial distance between resonances of the two features is controlled by the ratio $\Omega = \Omega_s/\Omega_b$, this ratio crucially controls chaoticity in the Galactic disk. We set up 4 distinct Milky Way models at 4 different values of Ω. One value of Ω is chosen to cause the resonances due to the bar and spiral to physically overlap while 2 other Galactic models involve Ω values for which the two resonances lie outside each other's respective resonance widths. For the 4^{th} model, neither resonance overlap, nor rapid gradients of the perturber's gravitational field was included. The latter is ensured by excluding the spiral pattern of the Galaxy as a perturber. With these models, a quantification of chaos in the Milky Way disk was undertaken (Chakrabarty & Sideris, 2008). The results are shown in Figure 1; we find that without the spiral, the disk is not rendered chaotic. Also, the strength of chaos is nearly the same in all models that include the spiral, whether resonance overlap happens or not. This indicates the possibility that galactic systems are not neccessarily built of regular orbits and that for chaos to be induced resonance overlap is not imperative.

4 Non-linear probability mass distribution in phase space in external galaxy

The Milky Way example above indicated the possibility that the idea that galactic phase spaces are smooth, monolithic structures is a misplaced notion. The complexity manifest in the Galaxy is treated as general, to inspire a non-linear phase portrait in external galaxies too. Here, the effect of such a phase space structure on the estimation of $\rho(\mathbf{x})$ is discussed in the context of the example distant galaxy NGC 3379 (Chakrabarty 2009).

If in a general dynamical system, the data are sampled from the sub-space U of W, the estimate $f(\hat{\mathbf{w}}, t)$ will be prior-driven unless the dimensionality of the function space is reduced to be $\leq$ that of the data space, as in any inverse problem. However, if the system admits only vague priors, dimensionality reduction will be demanded. Additionally, the simultaneous estimation of $g(\mathbf{x}, \mathbf{v}, t)$ could be achieved if $g(\cdot)$ could be embedded into the structure of $f(\cdot)$; this could be done by invoking the dependence of $f(\cdot)$ on a functional ψ of $\rho(\cdot)$, i.e. $f = f(\psi[\rho], \mathbf{w}, t)$.

The above situation is very much the essence of the application to galaxies as dynamical systems. To enhance sparsity in the models, first we slap stationarity on the unknowns, thus reducing the problem to a stationary inverse problem though the general Bayesian inferrential framework presented in Chakrabarty (2009) supports the learning of $f(\mathbf{w}, t)$ and $g(\mathbf{x}, \mathbf{v}, t)$. We also suggest a velocity independent evolution, which is acceptable for the collisionless system that a galaxy is. Next, we approximate the triaxial geometry of the system (astronomical literature suggests an ellipsoidal geometry) with a spherical one, i.e. assume the gravitational mass density is $\rho(r)$, where $r^2 = \sum_{i=1}^{3} x_i^2$. Next, using the governance of the phase space density by the Vlasov equation (in the gravitational case), we express $f(\mathbf{w})$ as a function of the integrals of motion K_i, $i = 1, 2, \ldots$. In fact, we choose to describe f by only 2 such integrals of motion, keeping the constraint on dimensionality of function space in mind. These integrals are chosen to expand the scope of modelling non-linearlities in phase space, such as anisotropy, which is acknowledged by the dependence of f on the particle angular momentum L. For the k^{th} particle, angular momentum is $L_k = \mathbf{x}_k \wedge \mathbf{v}_k$; the asymmetric dependence on the components of $\mathbf{x}$ and $\mathbf{v}$ acknowledges anisotropy. The other integral of motion is the total energy E : for the k^{th} particle $E_k = \Phi[\rho(r_k)] + \sum_{i=1}^{3}(v_i^{(k)})^2$, where $\Phi(r)$ is the gravitational potential energy, a functional of $\rho(r)$ as dictated by Gauss' Law.

Writing $f(E, L)$ is thus conducive to the embedding of one unknown - $\rho(r)$ - into the structure of the other unknown, $f(\cdot)$. Thus, we are now ready to perform estimation of both the uknown functions. This is attempted by first projecting $f(E[\rho(r_k), \mathbf{v}_k], L(\mathbf{x}_k, \mathbf{v}_k))$ into the manifold $U \subset W$ from which the data is sampled. Thus, if x_1, x_2, , v_3 are measured for the k^{th} particle, then

$$\nu(x_1^{(k)}, x_2^{(k)}, v_3^{(k)}) = \int f(E[\rho(r_k), \mathbf{v}_k], L(\mathbf{x}_k, \mathbf{v}_k)) dx_3^{(k)} dv_1^{(k)} dv_2^{(k)} \qquad (1)$$

For this integral to be computed, we need to establish the mapping χ : $E, L \longrightarrow W/U$. Such can be achieved using Stoke's theorem.

The likelihood is written as $\mathcal{L} = \mathcal{L}' \circ \eta(v_3|\sigma_\delta)$, where $\eta(v_3|\sigma_\delta)$ is the distribution of the measurement uncertainties in v_3. We can neglect the same for x_1 and x_2. The error distribution is given by astronomers and assumed normal with 0 mean and a dispersion σ_δ that is again provided by astronomers for the given observational apparataus. Here "$\circ$" denotes convolution of $\mathcal{L}'$ and $\eta(\cdot)$. This is how measurement errors are incorporated into the estimation. Also, assuming that the data are *i.i.d.*, $\mathcal{L}' = \prod_{k=1}^{N} \nu_k(x_1^{(k)}, x_2^{(k)}, v_3^{(k)})$.

Once the likelihood $\mathcal{L}$ is computed, it is used to write the joint posterior probability of the unknowns, given the data, i.e. $\Pr(f(\cdot), \rho(\cdot)|\{x_1^{(k)}, x_2^{(k)}, v_3^{(k)}\}_{k=1}^{N})$, using truncated normal priors. We sample from this high dimensional posterior using an adaptive Metropolis-Hastings (Haario et. al, 2005).

An application of this methodology to samples $\mathcal{D}_1$ and $\mathcal{D}_2$, of 2 different types of galactic particles in the galaxy NGC 3379 was performed by Chakrabarty (2009). The findings suggest that estimates for $\rho(r)$ from the two data sets are significantly different, over an extended range in r. This implies 2 distinct gravitational mass density structures for the same galaxy, which is of course impossible - this dichotomous result is thus incompatible with the information about our system and stems from an erroneous model assumption. Assuming stationarity in $f(\cdot)$ and $\rho(\cdot)$ and having tested for sphericity, the erroneous assumption is identified as both data sets being drawn from the same stochastic region of W that is defined by a given function of particle E and L. Such an assumed unique function is impossible if the galactic phase space comprises regions that do not communicate with each other and $\mathcal{D}_1$, $\mathcal{D}_2$ have been sampled from such disjoint stochastic volumes of W. Such isolated regions of W can exist for different reasons, but the easist way of ensuring such a phase space structure is if the system gravitational potential $\Phi(r)$ is bistable.

The ramification of such a phase space structure is that $\hat{\rho}(r)$ estimates based on data sets drawn from the isolated parts of W will in general not concur; also no such $\hat{\rho}(r)$ will be the galactic density. This underlies the fundamental risk involved in trying to perform estimation of $\rho(r)$ in a galaxy, without heeding to the inherent non-linearities in the galactic phase space. While having kinematic data from distinct particle populations is indicative of this, merging such kinematic data with independent measurement on a functional - say, $M[\rho(r)]$ - and its uncertainties ($M_0 \pm \delta M$) can be useful; such measurement, along with the uncertainties, could be incorporated into the modelling in different ways, for example by supplementing the aforementioned $\mathcal{L}'$ with the term $(M[\tilde{\rho}(r)] - M_0)/\delta M$, where the functional is computed using the density $\tilde{\rho}(r)$ that is the currently accepted density in the current step within Metropolis (Chakrabarty et. al, *under preparation*).

5 Summary

Galactic W is advanced as non-linear in general and the reason for this is suggested to be steep gradients in the potential, in addition to overlap of resonances of distinct dynamical components of the system. The effect of non-linearities in the galactic $f(\mathbf{w})$ might be to provide fallacious estimates of the system potential, when input data sets are sampled from distinct, isolated basins of attraction within W.

References

[1] D. Chakrabarty, *Different Tracers give Different Masses* (Warwick Statistics Tech report, i.e. CRiSM Working Papers Series (http://www2.warwick.ac.uk/fac/sci/statistics/crism/research/2009/paper09-47).

[2] D. Chakrabarty, *Astronomy* & *Astrophysics*, vol. 467, page 145 (2007).

[3] D. Chakrabarty & Sideris, I., *Astronomy* & *Astrophysics*, vol. 488, page 161 (2008).

[4] H. Haario, E. Saksman & J. Tamminen, *Computational Statistics*, vol. 20, page 265 (2005). .